# Factors Influencing the Cold-Season Diurnal Temperature Range in the United States

IMKE DURRE AND JOHN M. WALLACE

*Department of Atmospheric Sciences, University of Washington, Seattle, Washington*

(Manuscript received 27 October 2000, in final form 25 January 2001)

ABSTRACT

This study examines the contributions of sunshine duration, snow cover extent, and the atmospheric circulation to variations of the cold-season diurnal temperature range (DTR) in eight regions of the contiguous United States. The goal of the research is to facilitate the interpretation of long-term changes in the DTR in light of the possible anthropogenic role in these trends. For the cold seasons (Nov–Mar) between 1958/59 and 1994/95, daily surface observations at more than 200 stations from the First Summary of the Day (FSOD) dataset as well as selected daily fields from the NCEP–NCAR 40-Year Reanalysis Project are analyzed using compositing, correlation, and regression techniques. For each region, a sea level pressure anomaly pattern is identified that is linearly related to daily variations in the DTR. It is found that the presence of positive sea level pressure anomalies over a region, clear skies, and the absence of snow on the ground all favor high values of the regionally averaged DTR. The strength of these associations varies geographically because of the effects of nonlinear relationships, the frequency of snow cover, and the complexity of local dynamics.

The cold-season trends of several variables for the period 1965/66–1994/95 are also analyzed. During the 30-yr period of record, the central and southern United States experienced a decrease in the DTR, while the northeast, Pacific coast, and portions of the interior west experienced an increase. Variations in the DTR-related sea level pressure patterns and sunshine duration explain significant fractions of the DTR increase in the coastal Northwest and the DTR decrease in the south-central states. The DTR trends over the rest of the country are largely unrelated to linear trends in sunshine duration, snow cover, or the sea level pressure field. The spatial pattern of DTR trends is reproduced when homogeneity-adjusted data from the Global Historical Climatology Network are used in lieu of FSOD data. Hence, it appears that the geographical pattern of trends is not a result of inhomogeneities in the FSOD data. The findings presented here suggest that many of the observed cold-season trends in the DTR are not induced by linearly related changes in the atmospheric circulation and, therefore, are attributable either to internal nonlinear relationships in the climate system or to anthropogenic factors such as urbanization and increasing concentrations of greenhouse gases and tropospheric aerosols.

## 1. Introduction

Variations in the diurnal temperature range (DTR) tend to occur as a result of fluctuations in the surface radiative, latent, and sensible heat fluxes. During the cold season, changes in the large-scale atmospheric circulation can alter these fluxes through their influence on boundary layer structure, cloudiness, and snow cover. In view of the large variations and shifts in circulation patterns that have taken place during the second half of the twentieth century (e.g., Mantua et al. 1997; Thompson and Wallace 1998), it is conceivable that the atmospheric circulation could play a significant role in both interannual variations and long-term trends of the cold-season DTR.

The DTR has decreased over much of the globe during the past few decades (Karl et al. 1993b; Horton 1995; Easterling et al. 1997). However, some regions, such as the British Isles, the Iberian Peninsula, India, central Canada, and certain coastal areas of North America, have experienced increases in the DTR. Many of these trends have been accompanied by variations in cloud cover that are physically consistent with the DTR changes (Karl et al. 1987; Plantico et al. 1990; Karl et al. 1993b; Dai et al. 1997, 1999). Cloudy days are usually characterized by a low DTR, mainly because clouds limit the amount of net radiation at the surface and inhibit the rise of surface air temperature during the day by reflecting solar radiation more efficiently than most surfaces (Plantico et al. 1990; Robinson 1992; Karl et al. 1993b; Dai et al. 1997, 1999). Clouds also affect surface temperatures by trapping outgoing longwave radiation (Hansen et al. 1995; Mearns et al. 1995; Stenchikov and Robock 1995; Campbell and Vonder Haar 1997). The resulting tendency for nighttime temperatures to be warmer in the presence of clouds than under clear skies has led many scientists to speculate that this mechanism also contributes to a lowering of the DTR by clouds (Karl et al. 1984, 1987; Plantico et al. 1990; Hansen et al. 1995). However, recent theoretical and

*Corresponding author address:* Imke Durre, National Climatic Data Center, 151 Patton Avenue, Asheville, NC 28801.
E-mail: idurre@ncdc.noaa.gov

empirical studies indicate that the magnitude of the longwave cloud forcing does not vary with time of day (Mearns et al. 1995; Stenchikov and Robock 1995; Campbell and Vonder Haar 1997; Dai et al. 1999; Sun et al. 2000). As a result, clouds are unlikely to influence the DTR through their effect on the longwave radiation balance at the surface. Based on this evidence, it appears that the shortwave cloud forcing is the primary, if not the only, factor contributing to the relationship between the DTR and cloudiness.

Some studies have investigated the possibility that changes in snow cover extent over North America have contributed to the observed DTR trends (Cerveny and Balling 1992; Karl et al. 1993b), but collectively their findings have been inconclusive. The hypothesis of an association between trends in snow cover extent and the DTR is based on the fact that, because of the high albedo of snow, daytime temperatures tend to be lower over snow than over bare ground (Dewey 1977; Ruschy et al. 1991; Karl et al. 1993a,b; Leathers et al. 1995; Groisman et al. 1996; Hughes and Robinson 1996; Kalkstein et al. 1996). Snow also limits the heat flux exchange between the soil and the overlying air and thus permits nighttime surface air temperatures to drop more rapidly than under snow-free conditions (Dewey 1977; Karl et al. 1993b; Leathers et al. 1995). When a sufficient amount of solar radiation reaches the ground, the albedo effect is considerably more important than the effect of snow insulating the ground (Karl et al. 1993b; Leathers et al. 1995). Recent work by Groisman et al. (2000) and Sun et al. (2000) indicates that snow cover affects not only temperature itself, but also the relationship between cloudiness and temperature. Because the cloud albedo is generally closer in magnitude to the albedo of snow than to the albedo of bare ground, the influence of clouds upon daytime surface air temperature is reduced when the ground is blanketed with snow. Based on these findings, it appears that the DTR is generally depressed by the presence of snow, but that the magnitude of the depression may vary geographically and seasonally.

Relatively few studies of trends in the DTR have considered the possible contribution of changes in the atmospheric circulation to the DTR trends. Razuvaev et al. (1995) suggested that a decrease in November–March DTR over northern and central parts of the former Soviet Union between 1961 and 1990 may have been caused by an increase in the frequency of synoptic situations that favor warm advection and cyclogenesis. In agreement with this argument, Horton (1995) showed that the Siberian anticyclone was weaker during 1981–90 than during 1951–80, and Easterling et al. (1997) demonstrated that an index of surface westerlies based on the cold ocean–warm land pattern of Wallace et al. (1996) is negatively correlated with the DTR over a region stretching from northern Europe into Russia. Over the Iberian Peninsula, where precipitation tends to be suppressed when the westerlies over northern Europe are strong (Hurrell 1995; Thompson and Wallace 2000), Easterling et al. found positive correlations between the westerly index and the DTR.

Przybylak (2000) computed mean seasonal DTR over the Arctic for six different synoptic patterns and correlated mean wintertime Arctic DTR anomalies with the North Atlantic oscillation index and the zonal index. His results indicate that an increase in cyclonic activity over the Arctic that is associated with a more positive NAO index and stronger zonal flow over midlatitudes is partially responsible for the observed decrease in Arctic DTR during the winters of 1951–90.

By the same token, changes in the atmospheric circulation may have contributed to the trends in wintertime DTR over the United States. Based on a comparison of gridded DTR and sea level pressure anomalies for the 1981–90 period, Horton (1995) suggested that enhanced flow of continental or polar air may have accounted for at least a part of the increase in the DTR over the Great Lakes region and the west coast of the United States between the winters of 1951–80 and 1981–90. Such circulation changes might explain the fact that the Pacific Northwest has experienced an increase in the DTR and a decrease in cloudiness, whereas most of the contiguous United States has experienced a decrease in the DTR and an increase in cloudiness (Plantico et al. 1990; Karl et al. 1993b; Lettenmaier et al. 1994; Elliott and Angell 1997).

Studies of the relationship between total cloud cover over the United States and ENSO variability show that the warm phase of ENSO is associated with below-normal cloudiness over the Northwest and a tendency for above-normal cloudiness over the remainder of the country (Angell and Korshover 1987; Angell 1990; Kane and Gobbi 1995). Other researchers demonstrated that precipitation was suppressed over the Pacific Northwest and enhanced over parts of the southern United States during the positive polarities of the Pacific–North America pattern and Pacific decadal oscillation (PDO) that prevailed between the late 1970s and mid-1990s (e.g., Leathers et al. 1991; Mantua et al. 1997; Higgins et al. 2000). Croke et al. (1999), on the other hand, found cloudiness over selected regions of the United States to be better correlated with variations in the strengths of the climatological-mean surface anticyclones and cyclones than with large-scale circulation patterns. For example, cloud cover in the Northeast is negatively correlated with the strength of the Icelandic low, but poorly correlated with the North Atlantic oscillation because of a lack of an association with the Bermuda high. Croke et al.'s findings suggest that predefined teleconnection patterns may not always capture the full extent to which regional variations of a certain meteorological variable are related to the atmospheric circulation.

The main goal of this study is to determine to what extent cloudiness, snow cover, and local changes induced by the atmospheric circulation account for both the widespread downtrends in the DTR and regional

differences in DTR trends across the contiguous United States. A number of composite, correlation, regression, and linear trend analyses are performed on daily surface and lower-tropospheric data, focusing on the cold-season months (Nov–Mar) when the influence of teleconnection patterns on surface climate tends to be strongest. Employing simple linear regression, patterns of 1000-mb geopotential height (a surrogate for sea level pressure) are derived that explain the maximum possible fraction of the daily variance in the DTR. The configurations of these patterns as well as correlations between the associated circulation index time series and various meteorological variables provide information on the mechanisms by which the low-level circulation influences the regional DTR. The correlation analysis includes not only surface variables such as daily maximum and minimum temperatures, sunshine duration, and snow cover extent, but also the difference in temperature between the surface and 850-mb level that serves as a crude measure of the static stability of the atmospheric planetary boundary layer. The circulation index time series are also used to assess the contribution of the DTR-related height patterns to trends in regional cold-season DTR between 1965/66 and 1994/95. The distinction between this methodology and a correlation or regression analysis that involves indices of well-known circulation patterns, such as the Arctic oscillation, is that the configurations and spatial scales of circulation patterns are not determined a priori.

The paper is organized as follows. Section 2 describes the data and analysis techniques used in this study. The relationships between the DTR, sunshine duration, and snow cover in eight regions of the U.S. are documented in section 3. In Section 4, selected DTR-associated regional circulation patterns are presented, and their impact on the DTR is discussed. Trends in the DTR and the contributions of changes in sunshine duration and the 1000-mb height field to these trends are described in section 5. The paper concludes with a discussion and summary of the results in section 6.

## 2. Data and analysis techniques

### *a. Data*

The data used in this study include both daily surface station observations extracted from the First Order Summary of the Day (FSOD) dataset (France 2000), selected twice-daily, daily mean, and monthly mean fields from the National Centers for Environmental Prediction–National Center for Atmospheric Research (NCEP–NCAR) reanalysis project (Kalnay et al. 1996), and homogeneity-adjusted monthly mean maximum and minimum temperatures at U.S. stations in the Global Historical Climatology Network (Peterson and Vose 1997). The period of study is 1958–95, which includes 37 cold seasons (Nov–Mar 1958/59–1994/95).

Of the 16 variables represented in the FSOD data, daily maximum and minimum temperatures ($T_{max}$ and $T_{min}$), percent of possible sunshine ($p_{sun}$), and snow depth are used. All temperatures are converted from integral degrees Fahrenheit to degrees Celsius and are rounded to the nearest 0.1°C. For each day and location, the DTR is calculated by subtracting $T_{min}$ from $T_{max}$. Observations reported before 1984 underwent a ''gross value check'' at the National Climatic Data Center; measurements taken since 1984 have been subjected to a more rigorous quality-control and editing procedure (France 2000). During the course of our analysis, we identified a few instances in which the daily maximum temperature was lower than the daily minimum temperature reported for the same day. In all such cases, both $T_{max}$ and $T_{min}$ were replaced by missing value flags.

Since the FSOD dataset does not contain information on cloud amount, $p_{sun}$ is used as a measure of cloudiness. The daily percent of possible sunshine is defined as the ratio of observed sunshine duration to the astronomically possible sunshine duration (i.e., the time between sunrise and sunset), assuming a smooth spherical earth (Hameed and Pittalwala 1989). Since the 1950s, sunshine duration has been measured with a photoelectric sunshine recorder whose measurements are adjusted by observers in order to compensate for lack of instrument sensitivity and the effects of complex terrain (Hameed and Pittalwala 1989; Karl and Steurer 1990). Thus, even though changes in observers and observing practices may affect long-term records of sunshine duration, the observations of this variable appear to be more objective than observers' reports of total cloud amount (Karl and Steurer 1990). Since the sunshine recorder reports sunshine whenever the amount of radiation it receives exceeds a fixed threshold, the instrument may record sunshine even when the sky is partially obscured by cirrus or convective clouds. Conversely, the presence of fog can decrease the sunshine duration when no clouds are present. Despite these potential differences, Angell (1990) found the annual anomalies of $p_{sun}$ and total cloud amount to be correlated at a level of $-0.86$, with the strength of the correlations exceeding $-0.90$ in autumn and winter. Therefore, $p_{sun}$ may be viewed as a suitable proxy for total cloudiness.

In order to be included in the study, a station must be located in the contiguous United States and must have ''high-quality'' records of both $T_{max}$ and $T_{min}$. A station's record of a particular variable is considered to be of high quality if measurements of the variable are available for each season and are reported on at least 90% of all days within the cold season during the period of record. These criteria yield a total of 213 stations in the contiguous United States. It is clear from the map of station locations shown in Fig. 1 that far fewer high-quality stations are located in the western half of the country than in the eastern half. As indicated by various types of circles, high-quality records of snow depth and $p_{sun}$ are available only at a subset of the stations shown. Furthermore, observations of $p_{sun}$ do not begin until

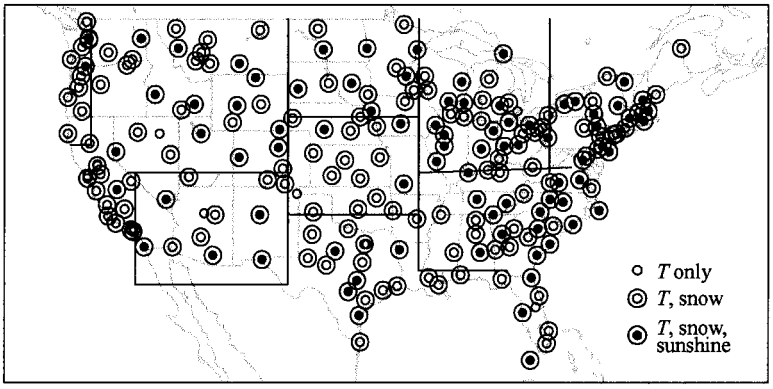


FIG. 1. Map of stations and regions used in this study. Region boundaries are indicated by solid lines. Open circles identify stations with high-quality records of daily maximum ($T_{max}$) and minimum ($T_{min}$) temperatures; closed circles identify stations with high-quality records of $T_{max}$, $T_{min}$, and percent of possible sunshine; concentric circles indicate the availability of a high-quality snow depth record in addition to the other data.

1965 in the FSOD dataset. The stations have been grouped into eight regions based on geographical homogeneity (Fig. 1). No region has been defined for the interior mountain west because of the paucity of stations and the large interstation variability in that part of the country.

The FSOD data have not been corrected for time-of-observation bias, station moves, instrument changes, or the effects of urbanization. Changes in observation time should not affect our results since the vast majority of the stations selected report observations for the 24-h period ending at midnight local time. Because of concerns about the effects of other inhomogeneities on the long-term trends computed in section 5, diurnal temperature range trends based on the FSOD data are compared with trends at stations in the Global Historical Climatology Network (GHCN). As described in Peterson and Vose (1997), the monthly mean maximum and minimum temperature data in the GHCN have been adjusted for discontinuities in time and space and consist mainly of data from rural stations. From this dataset, 1041 stations that are located in the contiguous United States and have high-quality temperature records have been selected.

Daily mean and monthly mean 1000-mb geopotential heights (m) as well as twice-daily (0000 UTC and 1200 UTC) 850-mb temperatures were extracted from NCEP–NCAR reanalysis files available at the National Oceanic and Atmospheric Administration–Cooperative Institute for Research in Environmental Sciences (NOAA–CIRES) Climate Diagnostics Center on a 2.5° × 2.5° latitude–longitude grid. A detailed description of the reanalysis data and possible sources of error can be found in Kalnay et al. (1996, as well as online at http://wesley.wwb.
noaa.gov/reanalysis.html). The difference in temperature between the surface and 850-mb level (TD) is used as a relative measure of boundary layer stability. For the morning hours, TD at a particular station is estimated by subtracting the 1200 UTC 850-mb temperature at the nearest grid point from the local daily minimum temperature. For the afternoon, the day's local maximum temperature and the next day's 0000 UTC 850-mb temperature are used to calculate TD. The morning and afternoon surface–850-mb temperature differences are denoted by $TD_{am}$ and $TD_{pm}$, respectively, and are computed only for stations at elevations below 700 m.

### *b. Basic analyses*

The limited availability of sunshine duration observations restricts all analyses that include $p_{sun}$ to the period 1965/66–1994/95 and to a subset of stations, as indicated in Fig. 1. Furthermore, because of the rare occurrence of snowfall in the southern states and coastal Northwest, stations in these regions are excluded from analyses involving snow depth.

Some of the analyses of this paper are performed on time series of regional-average values. Regional averages of $T_{max}$, $T_{min}$, the DTR, $p_{sun}$, $TD_{pm}$, and $TD_{am}$ are computed for eight regions (Fig. 1) by arithmetically averaging values from all stations within the region. A regional average for a particular day is formed only if data are available at more than 70% of the high-quality stations within the region. Otherwise, the day's regional average is considered as missing and is not included in any subsequent calculations. In the case of $TD_{pm}$ and $TD_{am}$, only stations at elevations below 700 m are included.

For each variable and each station, grid point, or region, time series of daily values are formed for the November–March season. Next, the seasonal cycle is removed from all time series by subtracting from each daily value the long-term mean for that date. When standardized values are required, the daily anomalies are divided by the standard deviation of all values in the time series.

*c. Derivation of DTR-related circulation patterns*

Patterns in the 1000-mb geopotential height field that are linearly related to variations in daily time series of the DTR have been computed on both a region-by-region and station-by-station basis. For this analysis, the 37 cold seasons (Nov–Mar) between 1958/59 and 1994/95, which comprise a total of 5596 days, are used.

For each of the eight regions outlined in Fig. 1, a regional 1000-mb geopotential height pattern associated with daily variations in the DTR is derived by regressing time series of daily geopotential height anomalies at each grid point within the North American sector (20°–60°N, 40°–140°W) onto a time series of daily standardized regional-mean DTR. Index time series that provide a measure of the temporal variations of the derived patterns are then formed by regressing daily maps of standardized geopotential heights onto a standardized version of each pattern. For the derivation of the circulation index time series of a particular region, only the portions of the 1000-mb height maps and regression pattern that fall within the area of the region of interest are used. The configuration of the patterns as well as the correlation of the index time series with the DTR, $p_{\text{sun}}$, and other meteorological variables are described in section 4 and are used to assess the statistical and physical significance of the patterns.

The dimensions of the domain used to derive the circulation index time series associated with each regional regression pattern were chosen based on the configuration of the pattern and experiments with domains of different sizes. When computing the circulation index for a particular region, using only the 1000-mb heights and regression coefficients within the region of interest yielded more consistent results than using a larger domain.

An analogous calculation of DTR-related 1000-mb height patterns has been carried out on a station-by-station basis. The station-by-station calculation permits the derivation of index time series of DTR-related variations in the 1000-mb height field for all available stations, including those located in data-sparse areas for which no analysis regions have been defined. For this purpose, time series of daily DTR anomalies at each station are used in place of regional-average time series. For the computation of the circulation index related to the DTR at a particular station, only the portion of the regression and 1000-mb height anomaly maps within a 10° latitude × 10° longitude box centered on the station are used. The dimensions of this area have been chosen based on the sizes of the eight analysis regions defined in Fig. 1 and a series of calculations in which the area of the box was varied (see section 5 below). The same station-by-station analysis has been performed using monthly mean maximum and minimum temperatures from 1041 GHCN stations and monthly mean 1000-mb heights from the NCEP–NCAR reanalysis.

*d. Correlations, trends, and residual trends*

Simple linear correlations and trends based on least squares regression are computed using time series of anomalies. The statistical significance of the correlation between two time series is tested with the *t* statistic, for which the number of independent samples is found by applying Leith's (1973) formula to both time series and choosing the smaller of the two resulting values. A correlation is considered to be meaningful if it is statistically significant at the 5% level. To test the statistical significance of the linear trend in a particular time series, the *t* statistic is applied to the correlation between the time series and time (that is, the sequence of dates associated with the time series), using the number of independent samples in the time series.

The linear contributions of $p_{\text{sun}}$ and DTR-related circulation indices to local and regional DTR trends have also been calculated and are discussed in section 5. If $b_{\text{sun}}$ (°C %$^{-1}$) and $b_{\text{circ}}$ [°C (standard deviation)$^{-1}$] are the slopes of the DTR-$p_{\text{sun}}$ and DTR-circulation index regression lines, and if $t_{\text{DTR}}$, $t_{\text{sun}}$, and $t_{\text{circ}}$ are the cold season trends in the DTR, percent of possible sunshine, and the circulation index, respectively, then the contributions $C_{\text{sun}}$ and $C_{\text{circ}}$ are computed as follows:

$$C_{\text{sun}} = b_{\text{sun}} \times t_{\text{sun}} \quad \text{and} \tag{1a}$$

$$C_{\text{circ}} = b_{\text{circ}} \times t_{\text{circ}}. \tag{1b}$$

The corresponding residual trends $R_{\text{sun}}$ and $R_{\text{circ}}$ are calculated according to the equations

$$R_{\text{sun}} = t_{\text{DTR}} - C_{\text{sun}} \quad \text{and} \tag{2a}$$

$$R_{\text{circ}} = t_{\text{DTR}} - C_{\text{circ}}. \tag{2b}$$

When compared with the overall DTR trends, the residual trends provide a quantitative estimate of the fraction of the trends that is not ''linearly congruent'' to the DTR-related circulation patterns or sunshine duration.

A frequently cited disadvantage of least squares regression is its sensitivity to outliers and end points. In addition, the underlying assumption that the variables to which the method is applied are normally distributed is frequently violated by daily values of meteorological variables in general and the diurnal temperature range and percent of possible sunshine in particular (Karl et al. 1993b; Lanzante 1996). In order to test for the importance of these factors in our results, we repeated some of our analyses using Pearson rank–order correlations as well as trends based on median of pairwise slopes regression (Lanzante 1996). These nonparametric techniques are resistant to outliers, do not emphasize the end points of time series, and do not require the variables to be normally distributed. To calculate the Pearson rank-order correlation between two time series *x* and *y*, the values of each time series are first ranked, and then the correlation coefficient between the resulting time series of ranks is computed. In median of pairwise slopes regression, the slope of the regression line is

TABLE 1. Correlations between daily anomalies of the diurnal temperature range and percent of possible sunshine during the cold season (Nov–Mar). Anomalies for 1965/66–1994/95 at all stations within a particular region are aggregated into a single set of station days. For each regional aggregate, correlations are computed for all station days (All), station days without snow on the ground (No SOG), and station days with a snow depth of at least 2.5 cm (SOG). The SOG–day correlation is computed only when at least 25% of all station days within a region are days with snow on the ground. Here *N* denotes the number of stations used.

| | | Correlation | | | % of days | |
|---|---|---|---|---|---|---|
| Region | *N* | All | No SOG | SOG | No SOG | SOG |
| Northeast | 13 | 0.39 | 0.41 | 0.35 | 65 | 35 |
| Midwest | 17 | 0.49 | 0.53 | 0.41 | 67 | 33 |
| Southeast | 12 | 0.60 | 0.60 | | 97 | 3 |
| Northern Plains | 7 | 0.44 | 0.57 | 0.34 | 43 | 57 |
| Southern Plains | 3 | 0.59 | 0.62 | 0.48 | 75 | 25 |
| South-central states | 5 | 0.69 | 0.69 | | 99 | 1 |
| Southwest | 5 | 0.58 | 0.58 | | 99 | 1 |
| Coastal Northwest | 2 | 0.60 | 0.61 | | 97 | 3 |

defined as the median of slopes between all possible pairs of points within the time series. Since this method necessitates the computation of $(N - 1)!$ slopes for a time series of length $N$, it was applied to time series of monthly averages rather than daily values. The correlations and trends obtained with the nonparametric methods turn out to be nearly identical in sign and similar in magnitude to those based on parametric techniques. Therefore, only the results based on the more widely used parametric techniques are shown. In general, the validity and importance of the trend in a particular variable are judged based on statistical significance, physical consistency with trends in other variables, and consistency with previously reported trends.

## 3. Regional DTR–cloudiness relationships and the influence of snow cover

Table 1 displays the cold-season correlation coefficients between daily anomalies of $p_{sun}$ and the DTR for each of the regions outlined in Fig. 1. These correlations are derived by first computing the daily anomalies of the DTR and $p_{sun}$ at each station and then correlating the anomalies for all station days between 1 November and 31 March within a region. The correlations between the DTR and $p_{sun}$, which are all statistically significant at the 99.9% level, demonstrate the strong relationship between cloudiness and the DTR. However, they also show that the association between the DTR and $p_{sun}$ is not as strong in the north-central and northeastern states as in other parts of the country. Dai et al. (1999) found cold-season correlations between the DTR and total cloud cover to be weaker at mid- and high latitudes in the Northern Hemisphere than at lower latitudes and attributed this result to the decrease in insolation with increasing latitude. This argument is supported by Sun et al.'s (2000) finding that the daytime cooling effect of clouds increases as the solar elevation angle increases. Thus, the north-to-south gradient in the DTR–$p_{sun}$ correlations east of the Rocky Mountains is consistent with a southward increase in insolation. In the western United States, however, the relationship between $p_{sun}$ and the DTR is as strong at coastal stations in the Pacific Northwest as in the Southwest, despite the meridional gradient in insolation.

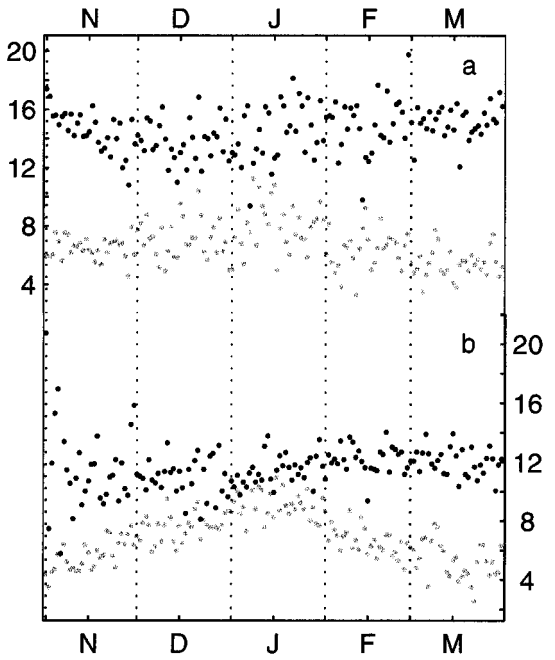


FIG. 2. Average diurnal temperature range (DTR, °C) in the northern Great Plains for clear (black) and cloudy (gray) days between 1 Nov and 31 Mar on which the ground is (a) snow-free (snow depth = 0) and (b) covered with at least 2.5 cm of snow. Days are defined as clear (cloudy) when the percent of possible sunshine is at least 90% (10% or less). Days between 1 Nov and 31 Mar are plotted on the abscissa; the DTR is plotted on the ordinate. Each dot represents an average over seven stations and the period 1965/66–1994/95 for a particular calendar day.

The relatively weak correlations between the DTR and $p_{sun}$ in the north-central and northeastern United States could also be an indication of the effects of snow cover since the influence of clouds on daytime surface air temperatures is reduced by the presence of snow on the ground (Groisman et al. 1994, 2000; Sun et al. 2000). Figure 2 shows seasonal variations of the DTR between 1 November and 31 March in the northern Great Plains for clear (black) and cloudy (gray) days on which either no snow is on the ground (top) or the snow depth equals at least 2.5 cm (bottom). A day is considered to be clear if $p_{sun}$ equals or exceeds 90%, while days with $p_{sun} \leq$ 10% fall into the cloudy category. The figure is constructed using observations at seven stations for the cold seasons of 1965/66–1994/95. Each dot in the figure represents a seven-station DTR average for one of the four categories of days on a particular calendar date.

It is evident from the top portion of Fig. 2 that on

TABLE 2. Average diurnal temperature range anomalies on clear and cloudy cold-season days with (SOG) and without (no SOG) snow on the ground. A day is defined as clear (cloudy) if the day's percent of possible sunshine is greater than or equal to 90% (less than or equal to 10%). Station data for the cold seasons of 1965/66–1994/95 are grouped into regional aggregates of station days as for Table 1.

| Region | No SOG | | SOG | |
|---|---|---|---|---|
| | Clear | Cloudy | Clear | Cloudy |
| Northeast | 1.69 | −2.01 | 1.50 | −1.96 |
| Midwest | 2.98 | −2.30 | 1.67 | −2.17 |
| Northern Plains | 3.61 | −3.81 | 1.26 | −2.74 |
| Southern Plains | 3.92 | −4.45 | 1.05 | −4.48 |

snow-free days throughout the cold season, the clear-sky DTR is higher than the cloudy-sky DTR. This relationship between the DTR and cloudiness is consistent with the results of Karl et al. (1987, 1993b), Plantico et al. (1990), and Groisman et al. (1996). In agreement with the findings of Groisman et al. (1994, 2000) and Sun et al. (2000), the difference in DTR between clear and cloudy days is less pronounced for days with snow on the ground, primarily because the clear-sky DTR is smaller. The DTR is least sensitive to both snow cover and cloudiness in midwinter when clear-sky solar radiation is at its minimum, as expected from analyses by Leathers et al. (1995) and Groisman et al. (1996).

In order to assess the extent to which snow cover influences the DTR–$p_{sun}$ relationship in different regions of the United States, correlations between the DTR and $p_{sun}$ have been computed separately for station days with no snow on the ground (no SOG) and for station days with a snow depth of at least 2.5 cm (SOG). These correlations, as well as the percentage of days in each of the two categories, are shown in Table 1. In addition, regional-average DTR anomalies have been calculated for the same four categories of days used to construct Fig. 2: clear no-SOG days, clear SOG days, cloudy no-SOG days, and cloudy SOG days (Table 2). The number of station days in each of the four categories used to construct Table 2 exceeds 2000 in all but two cases and ranges from 811 in the clear SOG group for the southern plains to 18 468 in the cloudy no-SOG category for the Midwest.

In every region in which both SOG and no-SOG categories are represented, the DTR–$p_{sun}$ correlation is higher without snow on the ground than in the presence of snow, although the association between the two variables is highly statistically significant for both categories of days (Table 1). The clear-sky DTR is consistently higher in the no-SOG category than in the SOG category, whereas the presence of snow appears to have little impact on cloudy-sky DTR (Table 2). These findings are consistent with a lowering of daytime temperatures due to the high albedo of snow (Groisman et al. 1996, 2000; Sun et al. 2000).

The depression of the overall correlation relative to the no-snow correlation is largest in the northern plains where fewer than one-half of the days are snow free, and the difference between the no-SOG and SOG correlations is largest. The Great Plains have previously been identified as the region of the United States in which the relationship between maximum temperature and snow cover extent is strongest (Dewey 1977; Karl et al. 1993a). The correlation on SOG days in the northern plains might be higher if it were not for the increase in DTR between cloudy snow-free days and cloudy SOG days. The relationship between the DTR and snow cover on cloudy days may be a result of a more rapid drop of nighttime temperatures over a snow-covered surface than over bare ground (Dewey 1977; Karl et al. 1993b; Leathers et al. 1995). Nevertheless the snow-related increase in the DTR on cloudy days does not offset the decrease on clear days. Both the correlations and average DTR anomalies indicate that in the southern plains, the DTR–$p_{sun}$ association remains relatively strong when snow is present, even though one might expect the more intense insolation in this region to enhance the albedo effect (Karl et al. 1993b). In comparison with the northern plains, more rapid melting between snowstorms in the southern plains is likely to decrease the snow albedo and, therefore, the impact of snow on daytime temperatures (Robock 1980; Leathers et al. 1995).

In the Northeast, the relationship between the DTR and cloudiness is relatively weak, regardless of whether snow is present. The difference between clear-sky and cloudy-sky DTR is barely larger without snow on the ground than in the presence of snow. Wagner (1973) and Leathers et al. (1995) found that the sensitivity of temperature to snow decreases toward the Atlantic coast, suggesting that the moderating influence of the ocean weakens the snow cover–temperature relationship. In addition, Robock (1980) noted that forested areas experience a much smaller snow-related change in surface albedo and daytime temperature than open, flat surfaces. Thus, both coastal influences and surface type may be responsible for the nearly negligible impact of snow cover on the DTR in the Northeast.

In summary, the presence of snow cover leads to a smaller clear-sky DTR in much of the central and northeastern United States. The relationship between the DTR and sunshine duration is most strongly affected by snow in the northern plains. The strength of the associations between the DTR, sunshine duration, and snow cover varies geographically depending on insolation, the frequency of snow cover and cloudiness, proximity to the ocean, and vegetation type. These findings will be taken into consideration where appropriate in the following sections.

## 4. DTR-related circulation patterns

In this section, 1000-mb geopotential height patterns associated with daily variations in regional DTR are examined and interpreted in the context of contempo-

raneous variations in other meteorological variables. Figure 3 displays a representative selection of the eight 1000-mb height regression patterns whose derivation is described in section 2c. The regression coefficient at each grid point represents the change in geopotential height (in meters) associated with a one standard deviation positive anomaly in regional DTR. Since, by definition, the patterns are linearly related to the regional DTR, a one standard deviation negative DTR anomaly is associated with 1000-mb height anomalies that are equal in magnitude but opposite in sign to those shown in Fig. 3.

Table 3 gives correlations between the daily index time series associated with each circulation pattern and anomalies of regional-average DTR, $p_{sun}$, $T_{max}$, $T_{min}$, $TD_{pm}$, and $TD_{am}$. Since the presence of snow cover can reduce the effect of variations in cloudiness on the DTR, it may also impact the relationship between the derived circulation patterns and the surface climate. For this reason, the correlations of the circulation pattern indices with the DTR and $p_{sun}$ for snow-free days are also calculated for the northern and southern plains, Midwest, and Northeast. A day is defined as snow free in a particular region if none of the stations with adequate snow depth data within the region report snow on the ground.

Among the correlations in Table 3, only those with magnitudes less than 0.08 are not significant at the 5% level. Thus, based on the correlations between the circulation indices and the DTR, all eight patterns are highly statistically significant. The significance of the patterns is further corroborated by the fact that very similar and physically consistent results are obtained when the same regression procedure is applied to 500-mb heights alone or to a combination of 500- and 1000-mb heights (not shown).

The regression patterns for the northeast and southeast are shown in Figs. 3a and 3b. A circulation pattern analogous to that for the Northeast is found to be associated with the DTR in the Midwest (not shown). In all three cases, the DTR is high when much of the region is located in the northern or northwestern quadrant of an anomalous surface anticyclone. The configuration of these patterns suggests that the depicted synoptic situation represents a transition from an anticyclonic to a cyclonic flow regime in the region of interest. This impression is confirmed by one-day lead and lag regression patterns (not shown) that show a progression of the high pressure center from west to east across the region. The patterns further imply that the affected region is dominated by an anomalous southwesterly to westerly low-level flow of relatively dry continental air. Conversely, a below-normal DTR is observed when easterly wind anomalies and relatively moist marine air prevail.

As can be seen from Table 3, the circulation index time series for the three regions are positively correlated with $TD_{pm}$, $T_{max}$, and $T_{min}$, negatively correlated with $TD_{am}$, and not well-correlated with $p_{sun}$. These correlations imply a tendency for the afternoon boundary

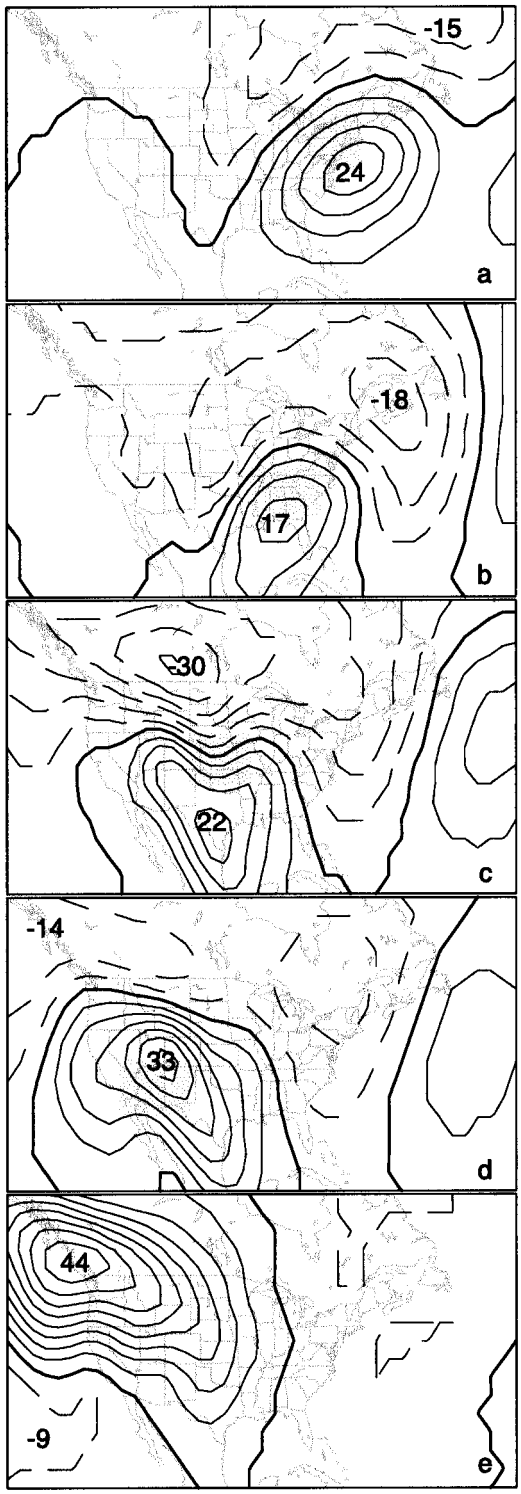


FIG. 3. DTR-related patterns of 1000-mb geopotential height anomalies for (a) the Northeast, (b) the Southeast, (c) the southern plains, (d) the Southwest, and (e) the coastal Northwest. Values are typical for a one standard deviation positive daily DTR anomaly during Nov–Mar. The contour interval is 5 m. Solid contours indicate positive height anomalies, dashed contours indicate negative anomalies, and the zero contour is thickened. In each panel, the pattern is related to the diurnal temperature range of the area shaded in gray.

TABLE 3. Daily correlations (decimal point omitted) between time series of DTR-related 1000-mb height patterns and other variables for the cold season (Nov–Mar). Variables include the daily maximum ($T_{max}$), minimum ($T_{min}$), and range (DTR) of surface air temperature, afternoon ($TD_{pm}$) and morning ($TD_{am}$) surface-to-850-mb temperature differences, and percent of possible sunshine ($p_{sun}$). Correlations are based on regional time series of daily anomalies. For DTR and $p_{sun}$ in the Northeast, Midwest, and Great Plains, correlations are shown for all days (All) and days with no snow on the ground (No SOG). The period 1958/59–1994/95 is used for all temperature variables; the period 1965/66–1994/95 is used for $p_{sun}$. Correlations greater than or equal to 0.08 are significant at the 5% level.

| | DTR | | $p_{sun}$ | | | | | |
|---|---|---|---|---|---|---|---|---|
| Region | All | No SOG | All | No SOG | $TD_{pm}$ | $T_{max}$ | $TD_{am}$ | $T_{min}$ |
| Northeast | 33 | 36 | −17 | −13 | 26 | 51 | −26 | 33 |
| Midwest | 37 | 39 | 19 | 22 | 39 | 33 | −22 | 15 |
| Southeast | 35 | | 05 | | 45 | 53 | −12 | 29 |
| Northern plains | 45 | 56 | 16 | 27 | 45 | 46 | −41 | 22 |
| Southern plains | 52 | 45 | 24 | 24 | 56 | 64 | −28 | 42 |
| South-central | 56 | | 43 | | 61 | 68 | −15 | 34 |
| Southwest | 45 | | 23 | | 03 | 20 | −42 | −20 |
| Coastal Northwest | 55 | | 54 | | −13 | −14 | −50 | −54 |

layer to be more unstable and the nighttime boundary layer to be more stable on days with above-normal DTR than on days with below-normal DTR. They further indicate that the positive polarity of the DTR-related circulation pattern tends to be associated with anomalously warm surface air temperatures.

Figure 3c shows the DTR-related pattern for the southern plains that is representative of the patterns obtained for all three regions of the central United States. In each case, the DTR tends to be high when positive 1000-mb height anomalies centered to the south of the region and a broad area of below-normal heights centered to the north act to produce anomalous westerly geostrophic flow over the region. These patterns are reminiscent of synoptic situations in which the region of interest is under the influence of a lee trough. The correlations between the circulation index time series and the DTR are larger than over the eastern United States and increase from 0.45 in the northern plains to 0.56 in the south-central states. The correlation between $p_{sun}$ and the corresponding DTR-related circulation index varies from 0.16 in the north to 0.43 in the south. When only days without snow on the ground are considered, the northern plains correlations are raised to levels comparable to those found in the southern plains, that is 0.56 for the DTR and 0.27 for $p_{sun}$. As in the eastern United States, the circulation indices for the central states are positively correlated with $TD_{pm}$, $T_{max}$, and $T_{min}$ as well as negatively correlated with $TD_{am}$.

These correlations suggest that the circulation patterns derived for the central United States affect the DTR to some extent by varying the strength of solar heating of the surface during the day. Schwartz and Skeeter (1994) found that continental air, which generally favors clear skies, dominates the north-central United States when a surface high is located over the center of the country. The conditions depicted in Fig. 3c and Table 3 may also be linked to adiabatic warming of Pacific air during its descent on the lee side of the Rocky Mountains (Kalkstein et al. 1996). When a central United States pattern is in its negative polarity, below-normal heights are found to the south of the DTR region, and upslope flow on the eastern side of the Rocky Mountains results in relatively cool, cloudy, low-DTR weather over the affected region in the central United States.

In the Southwest, a high DTR is associated with above-normal 1000-mb heights centered near the northern edge of the region (Fig. 3d). The configuration of the geopotential height field in Fig. 3d somewhat resembles synoptic-scale patterns that have been linked to subsidence and an absence of storms in the Southwest (Davis and Walker 1992; McCabe and Legates 1995). The time series of the Southwest circulation pattern is strongly negatively correlated with $TD_{am}$ (−0.42), weakly negatively correlated with $T_{min}$, and weakly positively correlated with $p_{sun}$ (0.23) and $T_{max}$ (0.20). The correlations imply that the positive polarity of the DTR-related pattern favors an unusually stable boundary layer at night, while the negative polarity favors less stable nighttime conditions.

The 1000-mb height pattern linked to above-normal DTR along the Pacific coast of the northwestern United States features strong positive anomalies centered approximately over Vancouver Island (Fig. 3e). This situation is favorable for fair weather over the Northwest as well as a Pacific storm track that is displaced northward or southward from its climatological-mean position (Skeeter and Park 1985; Leathers et al. 1991; Davis and Walker 1992; McCabe and Legates 1995). Daily variations in this circulation pattern are strongly positively correlated with the DTR (0.55) and $p_{sun}$ (0.54) and are negatively correlated with $T_{min}$ (−0.54) and $TD_{am}$ (−0.50). Thus, in comparison with the negative polarity, the positive polarity of this region's DTR-related circulation pattern is linked primarily to sunnier days and colder, more stable nights.

In summary, the DTR-related circulation patterns explain between 11% and 30% of the daily variance of the DTR in all regions. Figure 3 and Table 3 indicate that high (low) diurnal temperature ranges tend to occur in situations in which a high (low) pressure system is

centered over or near the area such that dry or continental (moist or marine) air is flowing over the region. Specifically, a high DTR is favored by westerly geostrophic winds near the surface in areas to the east of the Rockies and easterly winds in regions of the western United States.

The correlations between the circulation pattern indices and nighttime surface-to-850-mb temperature differences are negative across the entire country. To the east of the Rockies, the positive polarities of the patterns are associated with an anomalously unstable afternoon boundary layer as well as above-normal $T_{max}$ and $T_{min}$. The relationship between the circulation indices and $p_{sun}$ is strong only in the south-central states and coastal Northwest, suggesting that other, unidentified processes also contribute to the correlations between the circulation indices and the DTR. Considering the consistently negative correlations between $TD_{am}$ and the circulation indices, these processes may include those affecting the stability of the nighttime boundary layer. In the northern Great Plains, the index–DTR and index–$p_{sun}$ correlations improve when only snow-free days are considered (Table 3), since the presence of snow tends to weaken the relationship between the DTR and cloudiness (Tables 1 and 2).

When the analyses of this section are performed on monthly mean data, the resulting DTR-related circulation patterns (not shown) are qualitatively similar to those obtained from daily data. This finding suggests that the relationships between the circulation patterns and surface meteorological conditions described here are present not only at daily timescales, but also at monthly and longer timescales.

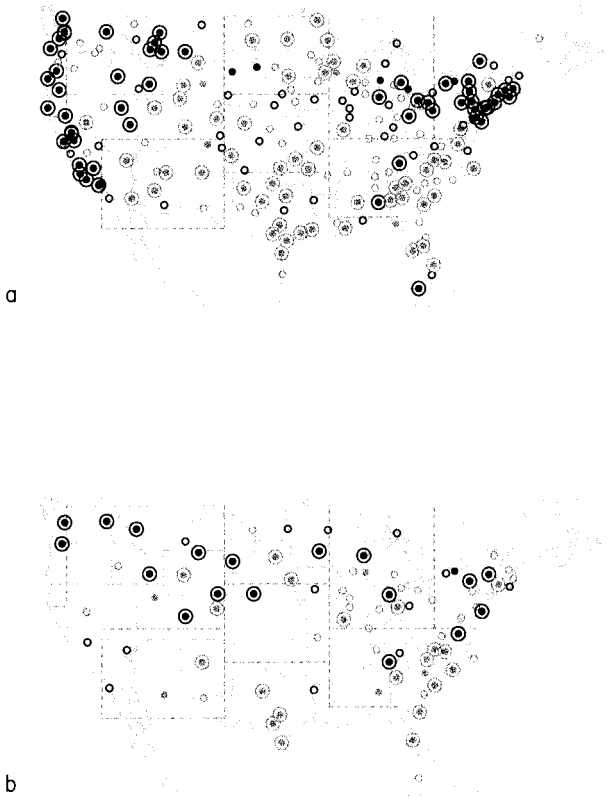


FIG. 4. Station trends of (a) the diurnal temperature range and (b) percent of possible sunshine for the cold seasons (Nov–Mar) of 1965/66–1994/95. Trends significant at the 5% (10%) level are marked by concentric (closed) circles. Trends not significant at the 10% level are marked by open circles. Positive trends are shown in black, negative trends in gray.

## 5. Observed cold-season DTR trends and contributing factors

In light of the results of the previous two sections, it appears that changes in cloudiness induced by changes in the atmospheric circulation could conceivably be contributing to long-term trends in the cold-season DTR. Karl et al. (1987, 1993b), Plantico et al. (1990), and Dai et al. (1997, 1999) have argued that much of the widespread decrease in the DTR since the 1950s can be attributed to an increase in cloudiness. An analysis of trends in the circulation pattern indices derived in the previous section should permit at least a preliminary assessment of the contribution of changes in the atmospheric circulation to the observed DTR trends. Since, in agreement with the work of Leathers et al. (1993), Brown et al. (1995), and Hughes and Robinson (1996), no notable changes in snow cover extent are found in the north-central and northeastern United States during the 1966–95 period (not shown), the linear contributions of snow cover extent to long-term changes in the DTR are considered to be negligible and will not be further analyzed during the course of this study.

Maps of observed linear trends in the DTR, percent of possible sunshine, and 1000-mb height for the 30 cold seasons between 1965/66 and 1994/95 are shown in Figs. 4 and 5. In addition, the 1965/66–1994/95 cold season trends of various variables have been calculated from time series for the eight regions outlined in Fig. 1 (Table 4). Trends significant at the 10% level are indicated by closed circles in Fig. 4. Trends significant at the 5% level are marked by concentric circles in Fig. 4 and are printed in bold in Table 4. In Fig. 5, the magnitudes of trends are indicated by geopotential height contours in order to facilitate a comparison of the pattern of 1000-mb height trends with the DTR-related circulation patterns shown in Fig. 3.

On a national scale, negative (gray) DTR trends dominate over positive (black) trends in Fig. 4a. Decreases in the DTR are found over the central and southern United States, although the regional-mean trends in the Great Plains and Southeast are not significant at the 5% level (Table 4). The Northeast, portions of the Northwest and northern Rockies, as well as some locations along the Gulf Coast have experienced an increase in the DTR, while the trends are of mixed sign in the Midwest. The DTR trends are accompanied by a considerable warming, with a larger rise in $T_{min}$ than in $T_{max}$ (Table 4). In

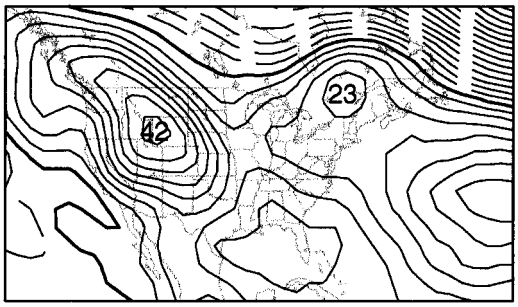


FIG. 5. Trends in 1000-mb geopotential height [m (30 yr)$^{-1}$] in the domain 20°–60°N, 40°–140°W for the cold seasons of 1965/66–1994/95. The contour interval is 10 m (30 yr)$^{-1}$. Solid contours indicate positive trends; dashed contours indicate negative trends, and the zero contour is thickened.

fact, $T_{min}$ has risen in all regions except the coastal Northwest, while $T_{max}$ has increased everywhere except over the south-central states.

Many previous analyses of DTR trends over the United States were based on periods of record beginning in the 1940s or early 1950s and ending in the 1980s or early 1990s (Karl et al. 1984, 1987, 1993b; Plantico et al. 1990; Lettenmaier et al. 1994; Knappenberger et al. 1996). Because linear trends are highly sensitive to the period of record chosen, a detailed comparison of Fig. 4a with the results of these earlier studies is difficult. In addition, differences in datasets and analysis techniques may contribute to disparities among the results. It is remarkable, however, that a preponderance of negative DTR trends over the United States as a whole and in the southern states in particular as well as the warming over the western states and northern plains are common to all of these studies. The wintertime cooling over the eastern United States that is noted in many of the earlier studies is present neither in our results nor in the results of Gaffen and Ross (1999) and Higgins et al. (2000) whose periods of record extend from the early 1960s through the early 1990s. A comparison of the cold season temperature trends for 1950–95 and 1966–95 in the GHCN dataset (not shown) indicates that the cooling trends are particular to the longer 1950–95 period, while a warming prevails over the eastern United States when the period of record is limited to 1966–95. Thus, the differences among previously published trends for this region can be attributed to the different periods of record used.

When compared with the trends in $T_{max}$ and $T_{min}$, the trends in the surface-to-850-mb temperature differences are less spatially coherent in sign and are generally smaller in magnitude (Table 4). Notable exceptions are found in the two western regions in Table 4. While both $TD_{pm}$ and $TD_{am}$ have decreased significantly in the coastal Northwest, they have increased significantly in the Southwest. The fact that, in the Pacific Northwest, the $TD_{pm}$ and $TD_{am}$ trends are negative and larger in magnitude than the $T_{max}$ and $T_{min}$ trends may be interpreted as indicative of a warming at the 850-mb level relative to the surface. Conversely, in the Southwest, the rise in surface air temperatures and surface-to-850-mb temperature differences could be viewed as a reflection of a warming of the surface relative to the 850-mb level that is particularly pronounced at night.

Trends in sunshine duration have been mostly downward over the southern United States and strongly upward at Pacific Northwest stations (Fig. 4b, Table 4). Over the remainder of the country, trends are small and vary in sign. These findings are qualitatively similar to those of many other studies of changes in cloudiness and/or sunshine duration (Karl et al. 1987; Angell 1990; Plantico et al. 1990; Kane and Gobbi 1995; Elliott and Angell 1997). In addition, the tendency toward less cloudy conditions at sites in the Pacific Northwest is in agreement with long-term decreases in precipitation over the region that have been reported by a number of researchers (e.g., Lettenmaier et al. 1994; Mantua et al. 1997; Higgins et al. 2000) and have been attributed to the 1976/77 jump in the Pacific decadal oscillation (Mantua et al. 1997; Higgins et al. 2000).

The spatial pattern of trends in the DTR (Fig. 4a) is physically consistent with the pattern of trends in $p_{sun}$ (Fig. 4b): areas of increases in the DTR are approximately collocated with areas of increasing sunshine duration, while areas of decreasing DTR are found where $p_{sun}$ has also been decreasing. Together with the rather strong, positive correlations between the DTR and $p_{sun}$

TABLE 4. Regional cold-season trends for 1965/66–1994/95. Variables include the DTR, daily maximum ($T_{max}$) and daily minimum ($T_{min}$) temperatures, afternoon ($TD_{pm}$) and morning ($TD_{am}$) surface-to-850-mb temperature differences, percent of possible sunshine ($p_{sun}$), and index time series of the DTR-related circulation patterns (Circ). Units are °C (30 yr)$^{-1}$ for all temperature variables, % (30 yr)$^{-1}$ for $p_{sun}$, and std dev (30 yr)$^{-1}$ for the circulation indices. Trends significant at the 0.05 level are printed in boldface type.

| Region | DTR | $T_{max}$ | $T_{min}$ | $TD_{pm}$ | $TD_{am}$ | $p^{sun}$ | Circ |
|---|---|---|---|---|---|---|---|
| Northeast | **0.7** | **1.7** | 1.0 | 0.2 | −0.4 | 0.9 | 0 |
| Midwest | 0.0 | **1.5** | **1.5** | −0.2 | −0.4 | −1.0 | 0.1 |
| Southeast | −0.6 | **1.2** | **1.9** | −0.4 | 0.1 | −5.8 | −0.2 |
| Northern Plains | −0.5 | **2.5** | **3.0** | −0.1 | 0.6 | 0.1 | 0.1 |
| Southern Plains | −0.4 | 0.8 | **1.3** | −0.2 | 0.5 | 2.5 | **−0.2** |
| South-central states | **−1.0** | −0.1 | 0.9 | **−0.8** | 0.2 | **−8.9** | **−0.3** |
| Southwest | **−1.2** | 0.6 | **1.7** | **0.8** | **2.2** | −2.3 | **0.5** |
| Coastal Northwest | **0.8** | 0.7 | −0.1 | **−1.0** | **−2.1** | **6.5** | **0.2** |

TABLE 5. Total and residual trends in regional-mean DTR for the cold seasons of 1965/66–1994/95. Here $R_{sun}$ denotes the residual trend after the contribution of percent of possible sunshine has been removed, and $R_{circ}$ denotes the residual trend after the contribution from the region's DTR-related circulation pattern has been removed. Trends significant at the 0.05 level are printed in boldface type.

| Region | Total | $R_{sun}$ | $R_{circ}$ |
|---|---|---|---|
| Northeast | **0.7** | **0.6** | **0.7** |
| Midwest | 0.0 | 0.1 | −0.1 |
| Southeast | −0.6 | −0.1 | −0.4 |
| Northern plains | −0.5 | **−0.5** | **−0.7** |
| Southern plains | −0.4 | **−0.8** | −0.1 |
| South-central states | **−1.0** | −0.1 | −0.4 |
| Southwest | **−1.2** | **−0.9** | **−1.8** |
| Coastal Northwest | **0.8** | **0.5** | **0.5** |

shown in Table 1, the similarity between the patterns of trends in Figs. 4a and 4b supports the conclusion of Karl et al. (1987), Plantico et al. (1990), and Dai et al. (1997, 1999) that changes in cloudiness are likely to have contributed significantly to the observed changes in the DTR.

The residual regional DTR trends ($R_{sun}$) obtained when removing the linearly congruent contribution of sunshine duration from the total regional 1965/66–1994/95 cold-season DTR trends are shown in Table 5. The removal of the variability due to $p_{sun}$ reduces the negative DTR trends over the south-central and southeastern states to near zero. In addition, the magnitudes of the negative trend in the Southwest and the positive trend in the coastal Northwest are decreased by 25% and 37.5%, respectively, but the trends of the residual DTR time series in those regions remain statistically significant. These findings suggest, in agreement with previous studies by Karl et al. (1987) and Plantico et al. (1990) that increases in cloudiness over the southern United States and decreases over the coastal Northwest contribute to the observed trends in the DTR. In the north-central and northeastern parts of the country, however, relatively low DTR–$p_{sun}$ correlations (Table 1) and/or negligible trends in $p_{sun}$ (Table 4) yield residual DTR trends that nearly equal the total DTR trends. Neither in these regions nor in the southern plains do the trends in the DTR during the cold season appear to be related to linear trends in sunshine duration.

The pattern of trends in 1000-mb heights in Fig. 5 indicates falling heights over parts of eastern Canada and the North Atlantic north of 50°N. Rising heights are found across the rest of the domain, with maxima over the northern Rockies and subtropical North Atlantic. The 1000-mb height patterns associated with variations in the DTR over the southern plains (Fig. 3c), south-central states (not shown), Southwest (Fig. 3d), and coastal Northwest (Fig. 3e) project, at least to some extent, onto the trends shown in Fig. 5. The tendency toward higher pressure over the Rocky Mountains is consistent with the 1976/77 shift in the PDO (Mantua et al. 1997), while the changes over the Atlantic are consistent with the trends in the Arctic oscillation and North Atlantic oscillation between the 1960s and 1990s (Hurrell 1995; Thompson and Wallace 1998).


FIG. 6. Contributions of DTR-related circulation patterns to station trends of the diurnal temperature range. A contribution to a station's DTR trend is based on a circulation index computed from 1000-mb heights within a (a) 5° × 5°, (b) 10° × 10°, and (c) 15° × 15° latitude–longitude box centered on the station. Two concentric circles represent a contribution that exceeds 5% of a station's mean cold-season DTR; a closed circle represents a contribution that exceeds 1% of a station's mean DTR; all smaller contributions are represented by open circles. Positive trends are shown in black, negative trends in gray.

Maps of the contributions ($C_{circ}$) of the DTR-related circulation pattern indices to the station DTR trends for "box sizes" of 5° × 5°, 10° × 10°, and 15° × 15° are shown in Fig. 6. Here, the box size limits the area around each station used to compute the DTR-related circulation index for that station (see section 2c). The contribution at each station is expressed as a percentage of the station's 1965/66–1994/95 cold-season DTR average. Although some differences among the three maps are apparent, the overall spatial pattern of the contributions remains qualitatively similar as the size of the

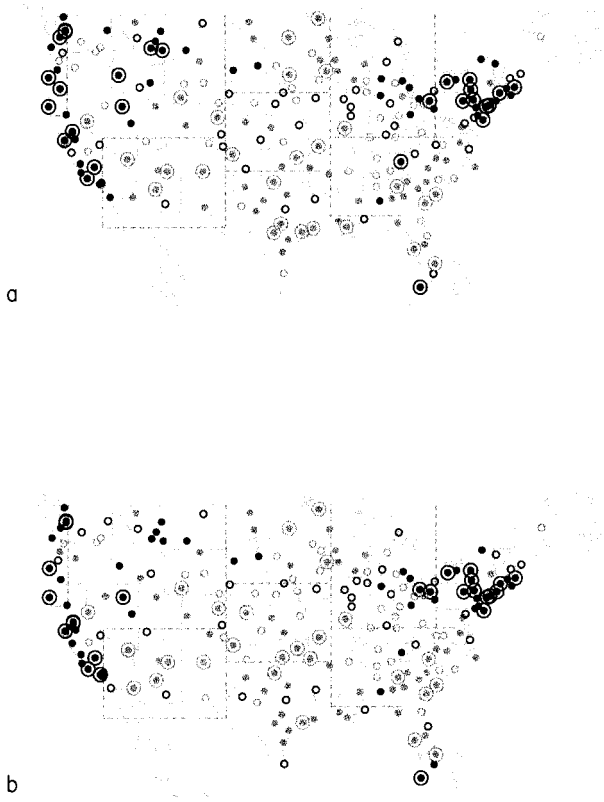


FIG. 7. (a) Diurnal temperature range trends for the cold seasons of 1965/66–1994/95 and (b) residual DTR trends following the removal of contributions from DTR-related circulation patterns, based on FSOD data. Two concentric circles represent a 30-yr trend that exceeds 10% of a station's mean cold-season DTR; a closed circle represents a trend that exceeds 5% of a station's mean DTR; all smaller trends are represented by open circles. Positive trends are shown in black, negative trends in gray.


FIG. 8. Diurnal temperature range trends based on data from the GHCN cold seasons 1965/66–1994/95. (a) Total 30-yr trends; (b) residual trends following the removal of contributions from DTR-related circulation patterns. The scale and plotting conventions are the same as in Fig. 7.

box around the station for which 1000-mb heights are included is increased. Circulation indices based on the intermediate box size of 10° × 10° are used when computing local residual DTR trends ($R_{\text{circ}}$) by removing $C_{\text{circ}}$ from the total trends in the DTR.

The total and residual station-by-station DTR trends for 1965/66–1994/95, again expressed as percentages of the DTR averages for the same period, are shown in Fig. 7 for the FSOD dataset and in Fig. 8 for the GHCN. In addition, the regional values of $R_{\text{circ}}$ are presented in Table 5. In contrast to the FSOD dataset, the GHCN consists mainly of rural stations whose data records have been adjusted for inhomogeneities (Peterson and Vose 1997). Therefore, the similarity of the spatial patterns in Figs. 7a and 8a indicates that the geographical distribution of the DTR trends cannot be attributed to inhomogeneities or a bias toward urban stations in the FSOD dataset. Judging from Table 5 and Figs. 7 and 8, the removal of the linearly congruent portions of the circulation pattern indices from the DTR time series has only a minor effect on the spatial pattern of DTR trends over the United States. Only in the south-central states and coastal Northwest do the DTR-related circulation indices consistently explain portions of the DTR trends. These two regions also happen to be the areas where significant trends in sunshine duration (Table 4) as well as strong correlations between the circulation indices and $p_{\text{sun}}$ (Table 3) are found.

In summary, the most coherent interrelationships among trends of different variables are found in the coastal Northwest where the increases in the DTR and daily maximum temperature are accompanied by physically consistent increases in sunshine duration, boundary layer stability, and 1000-mb geopotential heights. In the south-central United States, the trends in both sunshine duration and the DTR-related circulation index also are significant and of the same sign as the observed trend in the DTR. However, in contrast to the positive trends in the Northwest, the trends of the DTR, $p_{\text{sun}}$, and the DTR-related circulation index in the south-central region are negative. These observed long-term changes in 1000-mb heights, sunshine duration, and the DTR are all consistent with those expected in conjunction with the 1976/77 jump in the PDO.

## 6. Summary and discussion

In this study, relationships among the DTR, sunshine duration, snow cover, and the atmospheric circulation

during the cold season have been investigated. The conclusions drawn from these analyses may be summarized as follows.

1) In the northern plains and Midwest, the DTR under mostly clear skies is lower when snow is present than when the ground is snow free, while under cloudy conditions, the presence of snow affects the DTR to a much lesser extent (Table 2). As a result, the correlation between the DTR and sunshine duration is also lowered when snow covers the ground (Table 1). In the Northeast, where both the nearby ocean and forests may influence the local relationships among climate variables, the presence of snow has only a minimal effect on the DTR.
2) Circulation patterns associated with high (low) values of the DTR in a particular region feature positive (negative) 1000-mb height anomalies centered over or near the region, with a configuration that favors the flow of relatively dry continental (moist marine) air over the area of interest (Fig. 3).
3) For the cold seasons (Nov–Mar) of 1965/66–1994/95, negative DTR trends, which are concentrated in the central and southern United States, prevail over positive trends, which are found primarily in the Northeast, along the Pacific coast, and over northern portions of the interior West (Fig. 4a). A comparison of trends based on the FSOD data (Fig. 7a) and trends based on data from the GHCN (Fig. 8a) suggests that changes in instrumentation, station moves, and other spurious discontinuities do not contribute significantly to the DTR trends.
4) The observed negative DTR trend in the south-central United States and the positive DTR trend in the coastal Northwest appear to be partly associated with concomitant trends in sunshine duration and the 1000-mb height field (Tables 3–5, Figs. 4b and 7–8) which may, in turn, be linked to the 1976/77 shift in the Pacific decadal oscillation. The observed trends in the DTR over the remainder of the country do not appear to be linearly related to changes in sunshine duration, snow cover, or the atmospheric circulation.

Considering the nonlinearity of the relationships among the DTR, sunshine duration, and snow cover, it would be instructive to investigate changes in the DTR and snow cover extent on clear days only. A preliminary analysis with the present dataset indicates that on mostly sunny days ($p_{sun} \geq 75\%$), the DTR in the northern plains, Midwest, and Northeast increased, while snow cover extent decreased significantly in the northern plains and Northeast and slightly in the Midwest (not shown). This finding suggests a small positive contribution of snow cover to the DTR trends in these regions. However, in order to adequately assess the statistical significance and overall importance of this contribution, a longer period of record and a larger number of stations with the requisite data are needed.

As was pointed out by Kalkstein et al. (1996), correlations between synoptic-scale patterns and meteorological observations at the surface cannot be expected to be perfect since the same synoptic situations can result in a variety of surface conditions and vice versa. Furthermore, correlation analysis is a crude tool that reveals only simultaneous linear relationships when the causal links in nature may be more complex. A few nonlinearities are revealed in certain regions, for example, when composites of 1000-mb height anomalies for daily regional-mean DTR values that are more than one standard deviation above normal are compared with composites for DTR values that are more than one standard deviation below normal (not shown). The application of other techniques such as cluster analysis in future work may shed further light on synoptic-scale patterns that favor high or low values of the DTR. Last, the aggregation of data into regions and five-month seasons, while providing large samples for statistical analysis, may obscure certain relationships. Despite these limitations, our analysis has revealed some physically and statistically significant circulation patterns that are associated with variations in the DTR.

The fact that the analyses of section 5 leave the majority of the observed cold-season DTR trends unexplained implies either that the relationships between the DTR, sunshine duration, the atmospheric circulation, and snow cover extent are not adequately captured by linear analysis techniques or that factors not considered in this study contribute to the trends. Local and regional decreases in the DTR may be attributable to anthropogenic influences such as changes in land use and the rise in the concentrations of tropospheric aerosols and greenhouse gases.

The local effects of urbanization on surface air temperature are well documented (Cayan and Douglas 1984; Karl et al. 1988; Balling and Idso 1989; van den Dool et al. 1993; Gallo et al. 1996, 1999). Buildings and pavement tend to retain heat for a greater length of time than undeveloped, open landscape, resulting primarily in shallow surface warming at night. The urban heat island effect is expected to be particularly noticeable in the temperature trends of stations located in areas of rapid population growth such as the desert Southwest (Cayan and Douglas 1984), which has experienced the largest trend in $TD_{am}$ of the eight regions examined here (Table 4). On a national scale, decreases in the DTR also prevail at the mainly rural stations in the GHCN dataset (not shown), in agreement with previous work by Karl et al. (1988) and Gallo et al. (1999). Therefore, it appears that urbanization alone cannot account for the widespread DTR decreases. However, a contribution from other changes in land use/land cover (Gallo et al. 1996) that modify the energy balance at the surface cannot be ruled out.

Aerosols can raise the planetary albedo and serve as condensation nuclei, thus decreasing the intensity of daytime surface heating and possibly increasing the

amount of cloudiness (Charlson et al. 1992; Hansen et al. 1995; Karl et al. 1995; Dai et al. 1997). The influence of these mechanisms on local and regional DTR has yet to be investigated in detail.

Even though diurnal variations in the direct longwave radiative effect of atmospheric greenhouse gases on surface air temperature are believed to be small (Stenchikov and Robock 1995; Dai et al. 1999), the longwave radiative effects of an increase in greenhouse gases may alter nighttime boundary layer processes and, therefore, daily minimum temperatures under clear skies: the enhanced downward flux of longwave radiation from the atmospheric layer containing the increased concentrations of greenhouse gases would require a larger upward flux of longwave radiation from the earth's surface and, therefore, a warmer surface temperature. This primary effect is not expected to vary with time of day. However, the warmer surface could inhibit the formation of near-surface inversions during clear nights and thus slow the nighttime drop of surface air temperature. On the other hand, on clear days, the daily maximum temperature should be limited primarily by convective mixing with the overlying atmosphere and should therefore be largely unaffected by the radiative effects of a change in the concentration of greenhouse gases. Since water vapor is one of the greenhouse gases, an analysis of the relationship between the DTR, stability in the atmospheric boundary layer, and tropospheric water vapor under clear skies may be used in future work to assess the effect of increases in greenhouse gases on the frequency of nighttime inversions and the DTR.

*Acknowledgments.* We thank David Battisti, Conway Leovy, Dennis Lettenmaier, and the anonymous reviewers for their helpful suggestions. This work was supported by the National Science Foundation through the Climate Dynamics Program under Grant ATM-9805886. NCEP–NCAR reanalysis data were provided by the NOAA–CIRES Climate Diagnostics Center, Boulder, Colorado (http://www.cdc.noaa.gov/).

## REFERENCES

Angell, J. K., 1990: Variation in United States cloudiness and sunshine duration between 1950 and the drought year of 1988. *J. Climate,* **3,** 296–308.

——, and J. Korshover, 1987: Variability in United States cloudiness and its relation to El Niño. *J. Climate Appl. Meteor.,* **26,** 580–584.

Balling, R. C., Jr., and S. B. Idso, 1989: Historical temperature trends in the United States and the effect of urban population growth. *J. Geophys. Res.,* **94,** 3359–3363.

Brown, R. D., M. G. Hughes, and D. A. Robinson, 1995: Characterizing the long-term variability of snow-cover over the interior of North America. *Ann. Glaciol.,* **21,** 45–50.

Campbell, G. G., and T. H. Vonder Haar, 1997: Comparison of surface temperature minimum and maximum and satellite measured cloudiness and radiation. *J. Geophys. Res.,* **102,** 16 639–16 645.

Cayan, D. R., and A. V. Douglas, 1984: Urban influences on surface temperatures in the southwestern United States during recent decades. *J. Climate Appl. Meteor.,* **23,** 1520–1530.

Cerveny, R. S., and R. C. Balling Jr., 1992: The impact of snow cover on diurnal temperature range. *Geophys. Res. Lett.,* **19,** 797–800.

Charlson, R. J., S. E. Schwartz, J. M. Hales, R. D. Cess, J. A. Coakley Jr., J. E. Hansen, and D. J. Hofmann, 1992: Climate forcing by anthropogenic aerosols. *Science,* **255,** 423–430.

Croke, M., R. D. Cess, and S. Hameed, 1999: Regional cloud cover change associated with global climate change: Case studies for three regions of the United States. *J. Climate,* **12,** 2128–2134.

Dai, A., A. D. Del Genio, and I. Fung, 1997: Clouds, precipitation, and temperature range. *Nature,* **386,** 6651–6666.

——, K. E. Trenberth, and T. R. Karl, 1999: Effects of clouds, soil moisture, precipitation, and water vapor on diurnal temperature range. *J. Climate,* **12,** 2451–2473.

Davis, R. E., and D. R. Walker, 1992: An upper-air synoptic climatology of the western United States. *J. Climate,* **5,** 1449–1467.

Dewey, K., 1977: Daily maximum and minimum temperature forecasts and the influence of snow cover. *Mon. Wea. Rev.,* **105,** 1594–1597.

Easterling, D. R., and Coauthors, 1997: Maximum and minimum temperature trends for the globe. *Science,* **277,** 364–367.

Elliott, W. P., and J. K. Angell, 1997: Variations of cloudiness, precipitable water, and relative humidity over the United States: 1973–1993. *Geophys. Res. Lett.,* **24,** 41–44.

France, L., cited 2000: Summary of the Day—First Order—TD-3210. [Available online at http://www.ncdc.noaa.gov.]

Gaffen, D. J., and R. J. Ross, 1999: Climatology and trends of U.S. surface humidity and temperature. *J. Climate,* **12,** 811–828.

Gallo, K. P., D. R. Easterling, and T. C. Peterson, 1996: The influence of land use/land cover on climatological values of the diurnal temperature range. *J. Climate,* **9,** 2941–2944.

——, T. W. Owen, and D. R. Easterling, 1999: Temperature trends of the U.S. Historical Climatology Network based on satellite-designated land use/land cover. *J. Climate,* **12,** 1344–1348.

Groisman, P. Y., T. R. Karl, R. W. Knight, and G. L. Stenchikov, 1994: Changes of snow cover, temperature, and radiative heat balance over the Northern Hemisphere. *J. Climate,* **7,** 1633–1656.

——, E. L. Genikhovich, and P. M. Zhai, 1996: ''Overall'' cloud and snow cover effects on internal climate variables: The use of clear-sky climatology. *Bull. Amer. Meteor. Soc.,* **77,** 2065–2075.

——, R. S. Bradley, and B. Sun, 2000: The relationship of cloud cover to near-surface temperature and humidity: Comparison of GCM simulations with empirical data. *J. Climate,* **13,** 1858–1878.

Hameed, S., and I. Pittalwala, 1989: An investigation of the instrumental effects on the historical sunshine records for the United States. *J. Climate,* **2,** 101–104.

Hansen, J., M. Sato, and R. Ruedy, 1995: Long-term changes of the diurnal temperature cycle: Implications about mechanisms of global climate change. *Atmos. Res.,* **37,** 175–209.

Higgins, R. W., A. Leetmaa, Y. Xue, and A. Barnston, 2000: Dominant factors influencing the seasonal predictability of United States precipitation and surface air temperature. *J. Climate,* **13,** 3994–4017.

Horton, B., 1995: Geographical distribution of changes in maximum and minimum temperatures. *Atmos. Res.,* **37,** 101–117.

Hughes, M. G., and D. A. Robinson, 1996: Historical snow cover variability in the Great Plains region of the USA: 1910 through to 1993. *Int. J. Climatol.,* **16,** 1005–1018.

Hurrell, J. W., 1995: Decadal trends in the North Atlantic oscillation: Regional temperatures and precipitation. *Science,* **269,** 676–679.

Kalkstein, L. S., M. C. Nichols, C. D. Barthel, and J. S. Greene, 1996: A new synoptic classification: Application to air-mass analysis. *Int. J. Climatol.,* **16,** 983–1004.

Kalnay, E., and Coauthors, 1996: The NCEP/NCAR 40-Year Reanalysis Project. *Bull. Amer. Meteor. Soc.,* **77,** 437–471.

Kane, R. P., and D. Gobbi, 1995: Interannual variability of United States sunshine and cloudiness. *Ann. Geophys.,* **13,** 660–665.

Karl, T. R., and P. M. Steurer, 1990: Increased cloudiness in the United

States during the first half of the twentieth century: Fact or fiction? *Geophys. Res. Lett.,* **17,** 1925–1928.
——, G. Kukla, and J. Gavin, 1984: Decreasing diurnal temperature range in the United States and Canada from 1941 through 1980. *J. Climate Appl. Meteor.,* **23,** 1489–1504.
——, ——, and ——, 1987: Recent temperature changes during overcast and clear skies in the United States. *J. Climate Appl. Meteor.,* **26,** 698–710.
——, H. F. Diaz, and G. Kukla, 1988: Urbanization: Its detection and effect in the United States climate record. *J. Climate,* **1,** 1099–1123.
——, P. Y. Groisman, R. W. Knight, and R. R. Heim Jr., 1993a: Recent variations of snow cover and snowfall in North America and their relation to precipitation and temperature variations. *J. Climate,* **6,** 1327–1344.
——, and Coauthors, 1993b: A new perspective on recent global warming: Asymmetric trends of maximum and minimum temperature. *Bull. Amer. Meteor. Soc.,* **74,** 1007–1023.
——, R. W. Knight, G. Kukla, and J. Gavin, 1995: Evidence for radiative effects of anthropogenic sulfate aerosols in the observed climate record. *Aerosol Forcing and Climate,* R. J. Charlson and J. Heintzenberg, Eds., John Wiley and Sons, 363–382.
Knannenberger, P., P. Michaels, and P. Schwartzman, 1996: Observed changes in diurnal temperature and dewpoint cycles across the United States. *Geophys. Res. Lett.,* **23,** 2637–2640.
Lanzante, J. R., 1996: Resistant, robust, and non-parametric techniques for the analysis of climate data: Theory and applications, including applications to historical radiosonde station data. *Int. J. Climatol.,* **16,** 1197–1126.
Leathers, D. J., B. Yarnal, and M. A. Palecki, 1991: The Pacific/North American teleconnection pattern and United States climate. Part I: Regional temperature and precipitation associations. *J. Climate,* **4,** 517–528.
——, T. L. Mote, K. C. Kuivinen, S. McFeeters, and D. R. Kluck, 1993: Temporal characteristics of USA snowfall 1945–46 to 1984–85. *Int. J. Climatol.,* **13,** 65–76.
——, A. W. Ellis, and D. A. Robinson, 1995: Characteristics of temperature depression associated with snow cover across the northeast United States. *J. Appl. Meteor.,* **34,** 381–390.
Leith, C. E., 1973: The standard error of time-average estimates of climatic means. *J. Appl. Meteor.,* **12,** 1066–1069.
Lettenmaier, D. P., E. F. Wood, and J. R. Wallis, 1994: Hydro-climatological trends in the contiguous United States: 1948–88. *J. Climate,* **7,** 586–607.
Mantua, N. J., S. R. Hare, Y. Zhang, J. M. Wallace, and R. C. Francis, 1997: A Pacific interdecadal climate oscillation with impacts on salmon production. *Bull. Amer. Meteor. Soc.,* **78,** 1069–1079.
McCabe, G. J., Jr., and D. R. Legates, 1995: Relationships between 700-mb height anomalies and 1 April snowpack accumulations in the western USA. *Int. J. Climatol.,* **15,** 517–530.
Mearns, L. O., F. Giorgi, L. McDaniel, and C. Shields, 1995: Analysis of variability and diurnal range of daily temperature in a nested regional climate model: Comparison with observations and doubled $CO_2$ results. *Climate Dyn.,* **11,** 193–209.
Peterson, T. C., and R. S. Vose, 1997: An overview of the Global Historical Climatology Network Temperature Database. *Bull. Amer. Meteor. Soc.,* **78,** 2837–2849.
Plantico, M. S., T. R. Karl, G. Kukla, and J. Gavin, 1990: Is recent climate change across the United States related to rising levels of anthropogenic greenhouse gases? *J. Geophys. Res.,* **95,** 16 617–16 637.
Przybylak, R., 2000: Diurnal temperature range in the Arctic and its relation to hemispheric circulation patterns. *Int. J. Climatol.,* **20,** 231–253.
Razuvaev, R. N., E. G. Apasova, and R. A. Martuganov, 1995: Variations in the diurnal temperature range in the European region of the former USSR during the cold season. *Atmos. Res.,* **37,** 45–51.
Robinson, P. J., 1992: Trends in the relationship between monthly and daily temperatures across the United States. *Phys. Geogr.,* **13,** 191–205.
Robock, A., 1980: The seasonal cycle of snow cover, sea ice and surface albedo. *Mon. Wea. Rev.,* **108,** 267–285.
Ruschy, D. L., D. G. Baker, and R. J. Skaggs, 1991: Seasonal variation in daily temperature ranges. *J. Climate,* **4,** 1211–1216.
Schwartz, M. D., and B. R. Skeeter, 1994: Linking air mass analysis to daily and monthly midtropospheric flow patterns. *Int. J. Climatol.,* **14,** 439–464.
Skeeter, B. R., and A. J. Park, 1985: Synoptic control of regional temperature trends in the coterminous United States between 1949 and 1981. *Phys. Geogr.,* **6,** 69–84.
Stenchikov, G. L., and A. Robock, 1995: Diurnal asymmetry of climate response to increased $CO_2$ and aerosols: Forcings and feedbacks. *J. Geophys. Res.,* **100,** 26 211–26 227.
Sun, B., P. Y. Groisman, R. S. Bradley, and F. T. Keimig, 2000: Temporal changes in the observed relationship between cloud cover and surface air temperature. *J. Climate,* **13,** 4341–4357.
Thompson, D. W. J., and J. M. Wallace, 1998: The Arctic Oscillation signature in the wintertime geopotential height and temperature fields. *Geophys. Res. Lett.,* **25,** 1297–1300.
——, and ——, 2000. Annular modes in the extratropical circulation. Part I: Month-to-month variability. *J. Climate,* **13,** 1000–1016.
van den Dool, H. M., E. A. O'Lenic, and W. H. Klein, 1993: Consistency check for trends in surface temperature and upper-air circulation: 1950–1992. *J. Climate,* **6,** 2288–2297.
Wagner, A. J., 1973: The influence of average snow depth on monthly mean temperature anomaly. *Mon. Wea. Rev.,* **101,** 624–626.
Wallace, J. M., Y. Zhang, and L. Bajuk, 1996: Interpretation of interdecadal trends in Northern Hemisphere surface air temperature. *J. Climate,* **9,** 249–259.